Date of publication xxxx 00, 0000, date of current version xxxx 00, 0000.

Digital Object Identifier 10.1109/ACCESS.2017.DOI

Secondary Network Throughput Optimization of NOMA Cognitive Radio Networks Under Power and Secure Constraints

VAN NHAN VO[1,2], VIET-HUNG DANG[1,2], HUNG TRAN[3], DAC-BINH HA[4], CONG LE[5], TU DAC HO[6], AND CHAKCHAI SO-IN[7] (Senior Member, IEEE)

[1]Institute of Research and Development, Duy Tan University, Da Nang 550000, Vietnam (e-mail: vonhanvan@dtu.edu.vn and e-mail: dangviethung@duytan.edu.vn)
[2]Faculty of Information Technology, Duy Tan University, Da Nang 550000, Vietnam
[3]Faculty of Computer Science, Phenikaa University, Yen Nghia Ward, Ha Dong District, Hanoi 100000, Vietnam (e-mail: hung.tran@phenikaa-uni.edu.vn)
[4]Faculty of Electrical & Electronics Engineering, Duy Tan University, Danang 550000, Vietnam (e-mail: hadacbinh@duytan.edu.vn)
[5]Faculty of Computer Science, Vietnam Korea University of Information and Communications Technology, Danang University, Da Nang 550000, Vietnam (e-mail: ltcong@vku.udn.vn)
[6]Department of Electrical Engineering, Faculty of Engineering Science and Technology, UiT – The Arctic University of Norway (email: Tu.D.Ho@uit.no)
[7]Applied Network Technology (ANT) Laboratory, Department of Computer Science, College of Computing, Khon Kaen University, Khon Kaen 40002, Thailand (e-mail: chakso@kku.ac.th)

Corresponding author: Chakchai So-In (e-mail: chakso@kku.ac.th).

This work was supported by grants from Khon Kaen University, Thailand, and from the Artificial Intelligence Center (AIC), College of Computing, Khon Kaen University, Thailand. Dr. H. Tran has the same contribution as the first author.

ABSTRACT Recently, the combination of cognitive radio networks with the nonorthogonal multiple access (NOMA) approach has emerged as a viable option for not only improving spectrum usage but also supporting large numbers of wireless communication connections. However, cognitive NOMA networks are unstable and vulnerable because multiple devices operate on the same frequency band. To overcome this drawback, many techniques have been proposed, such as optimal power allocation and interference cancellation. In this paper, we consider an approach by which the secondary transmitter (STx) is able to find the best licensed channel to send its confidential message to the secondary receivers (SRxs) by using the NOMA technique. To combat eavesdroppers and achieve reasonable performance, a power allocation policy that satisfies both the outage probability (OP) constraint of primary users and the security constraint of secondary users is optimized. The closed-form formulas for the OP at the primary base station and the leakage probability for the eavesdropper are obtained with imperfect channel state information. Furthermore, the throughput of the secondary network is analyzed to evaluate the system performance. Based on that, two algorithms (i.e., the continuous genetic algorithm (CGA) for CR NOMA (CGA-CRN) and particle swarm optimization (PSO) for CR NOMA (PSO-CRN)), are applied to optimize the throughput of the secondary network. These optimization algorithms guarantee not only the performance of the primary users but also the security constraints of the secondary users. Finally, simulations are presented to validate our research results and provide insights into how various factors affect system performance.

INDEX TERMS Cognitive radio network, NOMA, Imperfect CSI, Throughput optimization, Performance constraints

I. INTRODUCTION

Recently, non-orthogonal multiple access (NOMA) in 3GPP has been regarded as a viable technology to increase not only spectrum usage but also support for many connections [1]–[7]. The key idea is that multiple NOMA users are able to access the same frequency at the same time [1]. Here, the transmitter may employ the superposition coding technique to combine multiple signals, while the receiver implements successive interference cancellation (SIC) to decode its signal [2]. The work reported in [7] showed that

the capacity of the NOMA approach is greater than that of orthogonal multiple access (OMA). Accordingly, NOMA has been employed for various systems, e.g., uplink/downlink transmission, two-way wireless networks, and cooperative cognitive radio network (CRN) [8]–[14]. Among those systems, CRN is widely regarded as an effective solution to the spectrum scarcity problem [14]. More specifically, in a CRN, a secondary user (SU) can communicate on a primary user (PU)'s licensed spectrum so long as it does not interfere with the communication of the PU [12]. Thus, by combining the architecture of CRN and NOMA, spectrum utilization will be improved significantly [11].

In [10], the authors surveyed three different cognitive radio (CR) NOMA architectures, i.e., underlay NOMA networks, overlay NOMA networks, and CR-inspired NOMA networks. The implementation of CR NOMA systems has been investigated in terms of open challenges and future research directions. In [15], the authors investigated the performance of a secondary network of a CR NOMA system servicing numerous users, in which a device-to-device (D2D) technique was used to enable signal transmission at close proximity to NOMA users. Given this context, an outage probability (OP) gap exists among the NOMA users that are studied to determine the system performance.

Furthermore, in [12], Do *et. al* studied a CR NOMA system to adapt to the requirements of 5G networks. The system performance in terms of OP for each NOMA was derived for Rayleigh fading channels. To capitalize on the benefits of cooperative communication, the authors devised a cooperative transmission method that takes advantage of the intrinsic diversity provided by CR NOMA [16]. The numerical results showed that the proposed CR NOMA system outperformed the CR OMA system because it increased the diversity orders of both the PU and SUs. In addition to the above benefits, the CRN increases the risk of wiretapping because this approach allows unlicensed users to share the same spectrum as licensed users. Thus, considering its broadcast nature, if the unlicensed users are untrusted, sensitive system information may be eavesdropped upon [17].

For instance, Y. Zou $et\ al.$ studied the CRN under wiretapping by an eavesdropper (EAV). They devised the closed-form formulas of the OP and leakage probability (LP) to examine the system and secrecy performance [18]. For multiple EAVss, in [19], N. Mokari $et\ al.$ explored the resilient resource allocation optimization problem for establishing secure transmission. Furthermore, in [20], the CR NOMA system was considered for two users in the presence of an EAV. The authors focused on how well the secrecy transmissions from the source node to the two users fared using the secrecy OP over Rayleigh fading channels. These works, however, did not take into account throughput optimization with a security constraint. Thus, to identify the optimal power allocation and achieve the highest possible throughput, many optimization techniques have been proposed. Specifically, optimization issues are resolved with the use of continuous genetic algorithms (CGAs) and particle swarm optimization (PSO) because PSO has a faster convergence time and the CGA can perform efficient exploration [21]–[25].

Nevertheless, to the best of our knowledge, no existing work on CR NOMA has studied joint constraints for an OP and LP to ensure that an EAV cannot monitor secret information while the primary base station (PBS) and secondary receivers (SRxs) can decode their signals. Accordingly, the following is a brief summary of the main points of this paper.

- We investigate a CR NOMA system in which multiple primary transmitters (PTxs) communicate with a PBS in the primary network while two SRxs, i.e., SRx_1 and SRx_2, receive a confidential signal from a secondary transmitter (STx) by using the NOMA principle in the presence of an EAV.
- We derive a closed-form formula for the throughput of the second network, i.e., from the STx to the SRxs, to evaluate the secondary network performance.
- We construct closed-form formulas for the OP at the PBS and the LP at the EAV to examine the primary network and secrecy performance, respectively.
- We apply and compare two algorithms (CGA for CR NOMA (CGA-CRN) and PSO for CR NOMA (PSO-CRN)) to optimize the secondary throughput with the constraint that the PBS can decode the signal from the selected PTx and the EAV cannot decode the STx's secret signal.
- We investigate the effect of the transmit power at the PTx and STx, the channel estimation error, and the channel mean gain on the secondary network throughput, primary OP, and LP.

II. RELATED WORK

In this section, a brief description of the use of the NOMA technique in a CRN is presented. To enhance the system performance, the authors of [16] presented a novel cooperative transmission scheme to exploit the inherent spatial diversity by using NOMA for a CRN. They constructed a closed-form formula for the OPs for SRxs to evaluate the system performance. Furthermore, the device-to-device transmission schemes for the CR NOMA system with two transmit sources and three users were investigated in [15]. The expressions of throughput and the OP were presented to confirm that the CR NOMA system works well with the device-to-device transmission ability. Notably, the imperfect channel state information (CSI) was taken into account in the CR NOMA system by the developers of [26]. They then derived the closed-form expression of the OP for each NOMA destination for the Rayleigh distribution to evaluate the system performance. However, these works did not take the security issue due to the EAV into account.

Therefore, the effects of multiple SUs selections on the secrecy performance of the PUs under a passive EAV were studied in [27]. The authors proposed a strategy based on the maximal jamming rate using NOMA and provided a closed-form formulation of the achievable ergodic secrecy rate. Based on the numerical findings, it was determined that the

proposed methods can considerably enhance the PUs's secret communication. Furthermore, the authors of [28] studied a secure CR NOMA system in which the transmitters delivered data to the recipients while shielding them from the EAVs. In particular, the considered model focused on a cognitive interference channel with an external EAV. Accordingly, the authors derived the achievable rate-equivocation region to examine the system performance. The numerical results then showed that the proposed secure NOMA-based scheme outperformed OMA by a wide margin. However, the aforementioned studies did not take into account the trade-off between secrecy and system performance.

Therefore, the trade-off between the OP and the secrecy OP of a CR NOMA system with multiple PUss and SUss was investigated in [17]. By pairing the PU and SU, the authors suggested a novel method of secure communication through NOMA. Accordingly, when the SUss are treated as the EAVs, closed-form equations for the OP and secrecy OP are obtained for primary users over Nakagami-m fading channels. The numerical results indicated that the secrecy performance may be enhanced by either lowering the number of SUss or combining the PUs with the best channel gains. Z. Xiang *et al.* presented a secure transmission scheme in hybrid automatic repeat request-assisted cognitive NOMA networks in the presence of an EAV, wherein a quality of service-sensitive user is viewed as a PU and a security-requiring user is treated as an SU to carry out NOMA. To reduce information leakage, the authors proposed a randomized retransmission NOMA (RR-NOMA) scheme by generating the retransmitted signals from independent randomized code books. Consequently, the closed-form formulations for the OP, secrecy OP, and throughput of the security-requiring user are determined to assess the system and secrecy performance [29].

However, according to the aforementioned survey, although the trade-off between the system performance and secrecy performance was surveyed in [17], [29], no previous publication has investigated the imperfect CSI and the constraints of the OP and intercept probability (IP) for the primary and secondary network of the CR NOMA system in the presence of an EAV. Therefore, in this research, we focus on these limitations to assess the system performance of the secondary network in the CR NOMA system.

For optimization after obtaining the closed form via system model analysis, most previous works apply the brute force method for only one parameter, as in [30], [31]. Generally, real-world objective functions are continuous, nonconvex, and multivariate, with a continuous search space and many constraints. Therefore, brute force is not suitable and should be replaced by other heuristic search methods. Some examples are simulated annealing (SA) [32], GA [24], PSO [25], the Bat Algorithm (BA) [33], and their variations for different types of problems. These methods initially perform random trials and then repeatedly utilize the results of the trials to generate better results. SA only allows one trial, or so-called candidate, at a time, while the other methods maintain a set of candidates as a population. Through the iterations, or generations, all candidates must exchange the explored information and collaborate with each other to produce a better set of candidates.

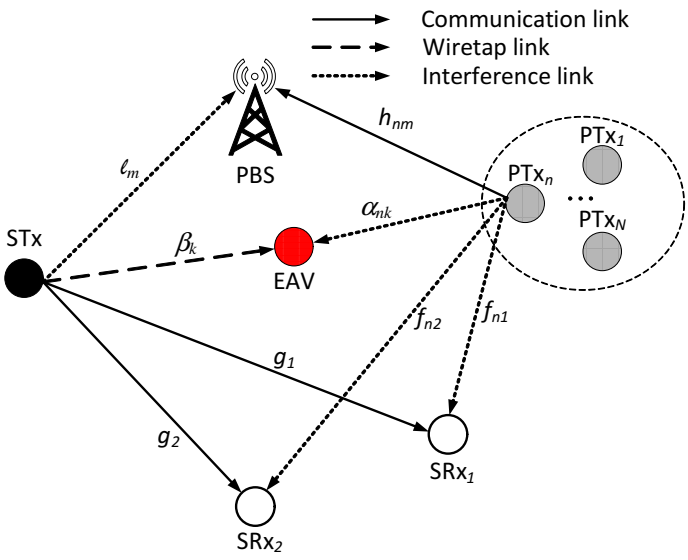

FIGURE 1: A system model of the CRN.

In our work, our derived closed form for throughput is not simply a convex function with only one optimum but is as complex as real-world problems. Moreover, it has many constraints and many local optima. Therefore, we will apply two heuristic methods, i.e., CGA, a GA variant for a continuous search domain, and PSO, to find the optimal P_P, P_S and μ_1. Both of these methods are appropriate for continuous-variable functions. Moreover, PSO provides fast convergence when the focus is on uphill climbing, while CGA performs a careful local search while allowing a certain probability of going downhill and random walking. After that, we present their convergence ability as well as the comparison before determining which one is better for our problem.

III. SYSTEM MODEL AND COMMUNICATION PROTOCOL

This section describes the framework of the system, including the channel assumptions and communication protocol.

A. SYSTEM MODEL

We consider a spectrum underlay CRN, as shown in Figure 1, in which multiple PTxs send information to a PBS by using the OMA principle, i.e., they do not cause mutual interference with each other [34]. A STx transmits its confidential signal to two SRxs, i.e., SRx$_1$ and SRx$_2$, by using the NOMA principle. There is also an EAV wishing to overhear the confidential signal from the STx. Note that the PBS and EAV are equipped with multiple antennas, while the remaining nodes (i.e., STx, PTxs, and SRxs) are assumed to have a single antenna [35], [36]. The main notation used to

describe the system model is listed in Table 1.

Here, all channel gains are independent and identically distributed (i.i.d.) and remain constant for the duration of one message, and they may be changed for the next one. It is noted that imperfect CSI of the channel gains $\chi \in \{g_1, g_2, \beta_k, h_{nm}, \alpha_{nk}, f_{n1}, f_{n2}, \ell_m\}$ is considered [3], [4], i.e.,

$$\chi = \hat{\chi} + e_\chi, \tag{1}$$

where $\hat{\chi} \in \left\{\hat{g}_1, \hat{g}_2, \hat{\beta}_k, \hat{h}_{nm}, \hat{\alpha}_{nk}, \hat{f}_{n1}, \hat{f}_{n2}, \hat{\ell}_m\right\}$ is the channel gain estimated by using the minimum mean squared error (MMSE) approach for χ; e_χ is the channel estimation error, and $e_\chi \sim \mathcal{CN}(0, \Omega_e)$.

In this work, it is assumed that there is no direct line of sight between the transmitter and receiver. Radio waves propagate through multiple paths and are subject to random phase shifts and amplitude attenuations caused by various factors, such as reflection, diffraction, and scattering. As a result, we assumed that the fading channel follows the Rayleigh model [36]. In this case, the channel gains are distributed as an exponential distribution function, and their probability density function (PDF) and cumulative distribution function (CDF) are written, respectively, as follows [35]:

$$f_{\hat{\chi}}(x) = \frac{1}{\Omega_{\hat{\chi}}} \exp\left(-\frac{x}{\Omega_{\hat{\chi}}}\right), \tag{2}$$

$$F_{\hat{\chi}}(x) = 1 - \exp\left(-\frac{x}{\Omega_{\hat{\chi}}}\right), \tag{3}$$

where the channel mean gain is $\Omega_{\hat{\chi}} = \mathbf{E}[\hat{\chi}]$.

TABLE 1: Notation

Notation	Definition
M	The number of antennas of the PBS
N	The number of PTx
K	The number of antennas of the EAV
g_φ	The channel gain from the STx to the φ-th SRx, where $\varphi \in \{1, 2\}$
β_k	The channel gain from the STx to the k-th antenna of the EAV, where $1 \le k \le K$
h_{nm}	The channel gain from the n-th PTx to the m-th antenna branch of the PBS, where $1 \le n \le N$ and $1 \le m \le M$
ℓ_m	The channel gain from the STx to the m-th antenna of the PBS
α_{nk}	The channel gain from the n-th PTx to the k-th antenna of the EAV
$f_{n\varphi}$	The channel gain from the n-th PTx to the φ-th SRx

B. COMMUNICATION PROTOCOL

The idea behind a spectrum underlay CRN is that the signals received from a PTx$_n$ at a PBS are distinct for each channel. Our suggested method is a centralized solution in which the ST hosts a centralized controller known as the CR network manager. Information is obtained by the PTx from the PBS and by the STx from the SRxs. The PTx and STx send their CSIs to the central controller, and this central controller uses finite-rate feedback connections [37]–[39] to send back some quantized CSIs to the PTx and STx. Thus,

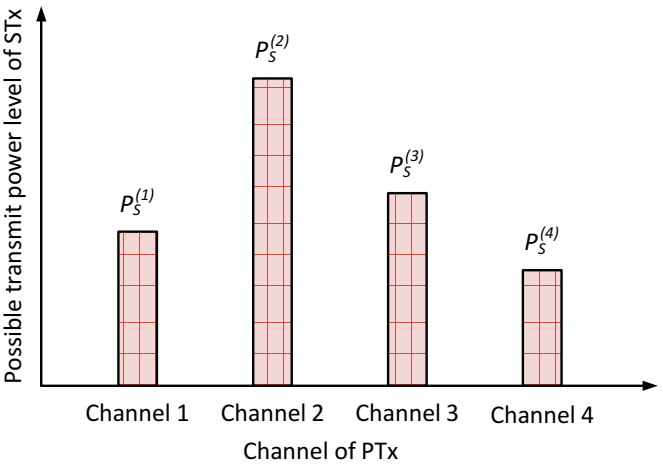

FIGURE 2: An example of the transmit power level of the STx at different channels of the multi-PTx.

once the STx knows the CSI of the PTx→PBS links, it can utilize the licensed spectrum of the PU and apply the NOMA principle to deliver the confidential signals to SRx$_1$ and SRx$_2$ without causing harmful interference for the PUs [40]–[42]. Intuitively, the PBS can tolerate different interference levels depending on the channel conditions between the n-th PTx and PBS. Thus, the STx can utilize the CSI to obtain different power allocation levels to reach the best performance. For example, in Figure 2, the transmit powers of the STx at channels 1, 2, 3, and 4 corresponding to the first, second, third, and 4-th PTx are $P_S^{(1)}$, $P_S^{(2)}$, $P_S^{(3)}$, and $P_S^{(4)}$, respectively.

We consider the case in which the transmission protocol is used in each time block [40]. As the STx utilizes the n-th channel of PTx$_n$ while PTx$_n$ communicates with the PBS, it generates limited interference for the PBS. Accordingly, the signal received at the m-th antenna of the PBS on the n-th channel can be expressed as

$$y_{nm} = \sqrt{P_P} h_{nm} x_P + \sqrt{P_S^{(n)}} \ell_m x_S + n_P, \tag{4}$$

where x_P and x_S are the signals of the n-th PTx and STx, respectively; P_P is the transmit power of the n-th PTx ($\forall n$); $n_P \sim \mathcal{CN}(0, N_0)$; and N_0 is the additive white Gaussian noise (AWGN). Accordingly, the received signal-to-interference-plus-noise ratio (SINR) at the m-th antenna of the PBS can be formulated as

$$\gamma_{nm} = \frac{P_P \hat{h}_{nm}}{P_S^{(n)} \hat{\ell}_m + P_P \Omega_e + P_S^{(n)} \Omega_e + N_0}. \tag{5}$$

Here, we assume that the PBSs employ the selection combining (SC) approach while decoding the signal sent by the n-th PTx [43]; thus, the SINR at the PBS can be expressed as

$$\gamma_n = \max_{m \in \{1, \cdots, M\}} \{\gamma_{nm}\}. \tag{6}$$

Additionally, the STx transmits the superimposed signal x_S to SRx_1 and SRx_2 with the interference generated by the n-th PTx

$$y_\varphi = \sqrt{P_S^{(n)}} g_\varphi x_S + \sqrt{P_P} f_{n\varphi} x_P + n_\varphi, \tag{7}$$

where $x_S = \sqrt{\mu_1} x_1 + \sqrt{\mu_2} x_2$, $\mu_1 + \mu_2 = 1$, and $\mu_1 < \mu_2$ [44]–[46]. Therefore, the signal received at the φ-th SRx can be rewritten as

$$y_\varphi = \sqrt{P_S^{(n)}} \left(\sqrt{\mu_1} x_1 + \sqrt{\mu_2} x_2\right) g_\varphi + \sqrt{P_P} f_{n\varphi} x_P + n_\varphi, \tag{8}$$

where $n_\varphi \sim \mathcal{CN}(0, N_0)$. It is noted that SRx_2 decodes signal x_2 by treating signal x_1 as noise. SRx_1 removes x_2 to obtain x_1 by adopting the SIC method [47]. Accordingly, the received SINRss at SRx_1 and SRx_2 used to decode signals x_1 and x_2 are expressed, respectively, as

$$\gamma_S^{(1)} = \frac{\mu_1 P_S^{(n)} \hat{g}_1}{P_P \hat{f}_{n1} + P_S^{(n)} \Omega_e + P_P \Omega_e + N_0}, \tag{9}$$

$$\gamma_S^{(2)} = \frac{\mu_2 P_S^{(n)} \hat{g}_2}{\mu_1 P_S^{(n)} \hat{g}_2 + P_P \hat{f}_{n2} + P_S^{(n)} \Omega_e + P_P \Omega_e + N_0}. \tag{10}$$

Furthermore, because of the broadcast nature of this method, the EAV also receives the signal from the STx and the n-th PTx as follows:

$$\begin{aligned} y_k =& \sqrt{P_S^{(n)}} \left(\sqrt{\mu_1} x_1 + \sqrt{\mu_2} x_2\right) \beta_k x_S \\ &+ \sqrt{P_P} \alpha_{nk} x_P + n_k, \end{aligned} \tag{11}$$

where $n_k \sim \mathcal{CN}(0, N_0)$. Similar to (9) and (10), the received SINRss at the k-th antenna of the EAV used to decode signals x_1 and x_2 are expressed, respectively, as

$$\gamma_{E_k n}^{(1)} = \frac{\mu_1 P_S^{(n)} \hat{\beta}_k}{P_P \hat{\alpha}_{nk} + P_S^{(n)} \Omega_e + P_P \Omega_e + N_0}, \tag{12}$$

$$\gamma_{E_k n}^{(2)} = \frac{\mu_2 P_S^{(n)} \hat{\beta}_k}{\mu_1 P_S^{(n)} \hat{\beta}_k + P_P \hat{\alpha}_{nk} + P_S^{(n)} \Omega_e + P_P \Omega_e + N_0}. \tag{13}$$

To improve the monitoring ability, the EAV uses antenna selection schemes as follows:

- Scheme $s1$: The selected antenna of the EAV is chosen so that the received SINR for detecting x_1 is maximal, i.e.,

$$\gamma_{En}^{(s1)} = \max_{1 \le k \le K} \left\{ \gamma_{E_k n}^{(1)} \right\}. \tag{14}$$

- Scheme $s2$: The selected antenna of the EAV is chosen such that the received SINR for detecting x_2 is maximal, i.e.,

$$\gamma_{En}^{(s2)} = \max_{1 \le k \le K} \left\{ \gamma_{E_k n}^{(2)} \right\}. \tag{15}$$

IV. PERFORMANCE ANALYSIS AND PROBLEM FORMULATION

In this section, the system performance of the secondary network is maximized while satisfying two constraints: 1) the system performance in terms of the OP of the n-th PTx to the PBS is not degraded; and 2) secure communication in terms of the LP of the STx to SRx_1 and SRx_2 is guaranteed.

A. PERFORMANCE ANALYSIS

We first derive the OP of the SU and then use it to calculate the throughput for analyzing the system performance. In particular, the OP of the second network is defined as either the channel capacity of the STx to the SRx_1 transmission link for decoding x_1 or that of the STx to the SRx_2 transmission link for decoding x_2 being lower than an outage target rate, R_S, i.e., [48]

$$\mathcal{O}_S = \Pr\left\{ C_S^{(1)} < R_S \text{ or } C_S^{(2)} < R_S \right\}, \tag{16}$$

where $C_S^{(\varphi)}$ is defined as

$$C_S^{(\varphi)} = W \log_2\left(1 + \gamma^{(\varphi)}\right). \tag{17}$$

Lemma 1. *The OP for the second network of both SRx_1 and SRx_2 is obtained as follows:*

$$\mathcal{O}_S = 1 - \left(1 - \mathcal{O}_S^{(1)}\right)\left(1 - \mathcal{O}_S^{(2)}\right), \tag{18}$$

where $\mathcal{O}_S^{(1)}$ and $\mathcal{O}_S^{(2)}$ are defined as

$$\begin{aligned} \mathcal{O}_S^{(1)} =& 1 - \frac{\mu_1 \rho_S^{(n)} \Omega_{\hat{g}_1}}{\Omega_{\hat{f}_{n1}} \theta_S \rho_P + \mu_1 \rho_S^{(n)} \Omega_{\hat{g}_1}} \\ &\times \exp\left\{ -\frac{\theta_S \left[\left(\rho_S^{(n)} + \rho_P \right) \Omega_e + 1 \right]}{\mu_1 \rho_S^{(n)} \Omega_{\hat{g}_1}} \right\}, \end{aligned} \tag{19}$$

$$\begin{aligned} \mathcal{O}_S^{(2)} =& 1 - \frac{\left(\mu_2 - \mu_1 \theta_S\right) \rho_S^{(n)} \Omega_{\hat{g}_2}}{\theta_S \rho_P \Omega_{\hat{f}_{n2}} + \left(\mu_2 - \mu_1 \theta_S\right) \rho_S^{(n)} \Omega_{\hat{g}_2}} \\ &\times \exp\left\{ -\frac{\theta_S \left[\left(\rho_S^{(n)} + \rho_P \right) \Omega_e + 1 \right]}{\left(\mu_2 - \mu_1 \theta_S\right) \rho_S^{(n)} \Omega_{\hat{g}_2}} \right\}. \end{aligned} \tag{20}$$

Proof: See Appendix A.

Accordingly, the expression for the throughput of the second network in the studied CR NOMA system is [49]

$$\mathcal{T}_S = \left(1 - \mathcal{O}_S\right) R_S. \tag{21}$$

Furthermore, given the analytical expressions, we have derived asymptotic expression for the considered system as the SNR go to infinity (i.e., $\mathcal{O}_{S,asymp} = \lim_{\rho_S^{(n)} \to \infty} \mathcal{O}_S$) as follows:

$$\mathcal{O}_{S,asymp} = \left(1 - \mathcal{O}_{S,asymp}^{(1)}\right)\left(1 - \mathcal{O}_{S,asymp}^{(2)}\right), \tag{22}$$

where $\mathcal{O}_{S,asymp}^{(1)}$ and $\mathcal{O}_{S,asymp}^{(2)}$ are defined as

$$\mathcal{O}_{S,asymp}^{(1)} = 1 - \exp\left\{ -\frac{\theta_S \Omega_e}{\mu_1 \Omega_{\hat{g}_1}} \right\}, \tag{23}$$

$$\mathcal{O}_{S,asymp}^{(2)} = 1 - \exp\left\{-\frac{\theta_S \Omega_e}{(\mu_2 - \mu_1\theta_S)\,\Omega_{\hat{g}_2}}\right\}. \quad (24)$$

Next, to guarantee the first constraint, we consider the case in which STx should allocate its power to keep the OP of the PBS below a predefined threshold, ε_B, i.e.,

$$\mathcal{O}_B = \Pr\{C_n < R_B\} \le \varepsilon_B, \quad (25)$$

where R_B is the target rate at the PBS, $\Pr\{\cdot\}$ is the probability function, and C_n is the channel capacity of the PTx$_n$→PBS link with the system bandwidth (W) as follows:

$$C_n = W \log_2(1 + \gamma_n). \quad (26)$$

To guarantee the second constraint, the LP at the EAV that can decode the confidential signal from the STx should be less than a leakage threshold, ε_E; i.e.,

$$\mathcal{O}_E^{(\varphi)} = \Pr\left\{C_{En}^{(\varphi)} \ge R_E\right\} \le \varepsilon_E, \quad (27)$$

where R_E is the outage target rate at the EAV and $C_{En}^{(\varphi)}$ is the channel capacity of the STx-EAV link for the signal x_φ as follows:

$$C_{En}^{(\varphi)} = W \log_2\left(1 + \gamma_{En}^{(\varphi)}\right). \quad (28)$$

To obtain the power allocation policies, we prove the following lemmas.

Lemma 2. *The first constraint, i.e.,* (25)*, is that the OP at the PBS of the information from the n-th PTx under interference from the STx is below ε_B, as follows:*

$$\mathcal{O}_B = \prod_{m=1}^{M}\left\{1 - \frac{\rho_P \Omega_{\hat{h}_{nm}}}{\theta_B \rho_S^{(n)} \Omega_{\hat{\ell}_m} + \rho_P \Omega_{\hat{h}_{nm}}} \times \exp\left\{-\frac{\theta_B\left[\left(\rho_P + \rho_S^{(n)}\right)\Omega_e + 1\right]}{\rho_P \Omega_{\hat{h}_{nm}}}\right\}\right\} \le \varepsilon_B. \quad (29)$$

Proof: See Appendix B.

Lemma 3. *The second constraint, i.e.,* (27)*, is that the LP for x_1 and x_2 at the EAV of the information from the STx is below ε_E for the two schemes, i.e., $(s1)$ and $(s2)$, as follows:*

$$\mathcal{O}_E^{(s1,1)} = 1 - \prod_{k=1}^{K}\left\{1 - \frac{\mu_1 \rho_S^{(n)} \Omega_{\hat{\beta}_k}}{\theta_E \rho_P \Omega_{\hat{\alpha}_{nk}} + \mu_1 \rho_S^{(n)} \Omega_{\hat{\beta}_k}} \times \exp\left\{-\frac{\theta_E\left[\left(\rho_S^{(n)} + \rho_P\right)\Omega_e + 1\right]}{\mu_1 \rho_S^{(n)} \Omega_{\hat{\beta}_k}}\right\}\right\} \le \varepsilon_E, \quad (30)$$

$$\mathcal{O}_E^{(s1,2)} = \frac{\rho_S^{(n)}(\mu_2 - \mu_1\theta_E)\,\Omega_{\hat{\beta}_k}}{\theta_E \rho_P \Omega_{\hat{\alpha}_{nk}} + \rho_S^{(n)}(\mu_2 - \mu_1\theta_E)\,\Omega_{\hat{\beta}_k}} \times \exp\left\{-\frac{\theta_E\left[\left(\rho_S^{(n)} + \rho_P\right)\Omega_e + 1\right]}{\rho_S^{(n)}(\mu_2 - \mu_1\theta_E)\,\Omega_{\hat{\beta}_k}}\right\} \le \varepsilon_E, \quad (31)$$

$$\mathcal{O}_E^{(s2,1)} = \frac{\mu_1 \rho_S^{(n)} \Omega_{\hat{\beta}_k}}{\theta_E \rho_P \Omega_{\hat{\alpha}_{nk}} + \mu_1 \rho_S^{(n)} \Omega_{\hat{\beta}_k}} \times \exp\left\{-\frac{\theta_E\left[\left(\rho_S^{(n)} + \rho_P\right)\Omega_e + 1\right]}{\mu_1 \rho_S^{(n)} \Omega_{\hat{\beta}_k}}\right\} \le \varepsilon_E, \quad (32)$$

$$\mathcal{O}_E^{(s2,2)} = 1 - \prod_{k=1}^{K}\left\{1 - \frac{\rho_S^{(n)}(\mu_2 - \mu_1\theta_E)\,\Omega_{\hat{\beta}_k}}{\theta_E \rho_P \Omega_{\hat{\alpha}_{nk}} + \rho_S^{(n)}(\mu_2 - \mu_1\theta_E)\,\Omega_{\hat{\beta}_k}} \times \exp\left\{-\frac{\theta_E\left[\left(\rho_S^{(n)} + \rho_P\right)\Omega_e + 1\right]}{\rho_S^{(n)}(\mu_2 - \mu_1\theta_E)\,\Omega_{\hat{\beta}_k}}\right\}\right\} \le \varepsilon_E. \quad (33)$$

Proof: See Appendix C.

B. PROBLEM FORMULATION

In this work, we maximize the throughput of the secondary network, i.e., $\mathcal{T}_S$, with two constraints: 1) the PBS can decode the signal from the n-th PTx, and 2) the EAV cannot wiretap the confidential signal from the STx. In particular, based on Lemmas 1, 2, and 3, the OP at the PR must be no larger than a predefined threshold, denoted by ε_B, and the LPs of the EAV for decoding the confidential signals must be less than a certain leakage threshold, denoted by ε_E. We aim to optimize the transmit power of the n-th PTx, the transmit power of the STx, and the NOMA power allocation factors. It is noted that this is a non-linear optimization problem because $\mathcal{T}_S$ has the component of $\mathcal{O}_S^{(1)}$ and $\mathcal{O}_S^{(2)}$. Thus, the optimization problem can be presented as

$$\max_{\mu_1, P_P, P_S^{(n)}} \{\mathcal{T}_S\}, \quad (34)$$

$$\text{s.t. } P_S^{(n)} \le P_{\text{peak}},$$
$$\mathcal{O}_B \le \epsilon_B,$$
$$\mathcal{O}_E^{(s1,1)} \le \varepsilon_E,$$
$$\mathcal{O}_E^{(s1,2)} \le \varepsilon_E,$$
$$\mathcal{O}_E^{(s2,1)} \le \varepsilon_E,$$
$$\mathcal{O}_E^{(s2,2)} \le \varepsilon_E.$$

where P_{peak} is the maximum transmit power of the STx.

V. CGA AND PSO ALGORITHMS FOR THE CR NOMA SYSTEM

The closed-form equations are necessary not only for designers who want to investigate how a system works with different configuring parameters but also for those who desire

to find the optimal working parameter set. These equations play the role of constructing an objective function for tuning the system parameters. In addition, the found closed forms tell us that the objective function is continuous and derivable, which is suitable for heuristic optimization methods.

In this work, we apply two heuristic methods for optimizing throughput to show that it is not just possible but also convenient to use heuristic methods for this throughput optimization problem. Generally, these two methods deploy a search with multiple solution candidates. Each candidate utilizes the information experienced by all candidates to evolve into its best form. The first method is the CGA-CRN, which is a variation of the GA designed for continuous search. Unlike traditional GA with bit strings for chromosomes, CGA-CRN considers a real vector for a set of optimizing variables. CGA-CRN also applies GA steps such as selection, crossover, and mutation. The selection step guarantees search convergence, while crossover and mutation play the roles of local search. The second method is PSO-CRN, inspired by a flock of animals finding prey. The members of the flock refer to a member with a high possibility of being near the prey and then adjust their speeds and positions to approach that member to increase the possibility of finding prey. In our work, we try to simultaneously find μ_1, P_P, and P_S to maximize the throughput under the set of constraints stated in (34). Therefore, we formulate the k-th candidate in the g-th generation as

$$\lambda_k^{(g)} = \left[\mu_1, P_P, P_S^{(n)}\right], \tag{35}$$

for both methods, where $\mu_2 = 1 - \mu_1$, $g \in \{1, \ldots, G\}$, and $k \in \{1, \ldots, Pop\}$, with G being the maximum number of generations of the methods and Pop being the population size or the number of candidates in each generation; note that with a given set of P_P and $P_S^{(n)}$, our model can determine which channel n is based on a predefined table (as illustrated in Figure 2). The fitness function is not the exact objective function throughput in (34) but the throughput with penalties to guarantee that the constraints are satisfied. Specifically, we propose a new fitness function as follows:

$$\begin{aligned} Fitness(\mu_1, P_P, P_S) &= \mathcal{T}_S - w_1 \max\left(P_S - P_{peak}, 0\right) \\ &- w_2 \max\left(\mathcal{O}_B - \epsilon_B, 0\right) - w_3 \max\left(\mathcal{O}_E^{(s1,1)} - \varepsilon_E, 0\right) \\ &- w_4 \max\left(\mathcal{O}_E^{(s1,2)} - \varepsilon_E, 0\right) - w_5 \max\left(\mathcal{O}_E^{(s2,1)} - \varepsilon_E, 0\right) \\ &- w_6 \max\left(\mathcal{O}_E^{(s2,2)} - \varepsilon_E, 0\right), \end{aligned} \tag{36}$$

where w_i are the positive weights so that the penalties are valid. If a constraint is violated, then the fitness value suffers the corresponding penalty with a lower value. Note that this fitness function is defined for both applied methods for the convenience of comparison.

The details of CGA-CRN and PSO-CRN are presented in Algorithm 1 and Algorithm 2, respectively. Both algorithms take the population size Pop and the limit number of generations G as input. For initialization, CGA-CRN needs the crossover rate r_c and mutation rate r_m as input, while PSO-CRN needs r_{local}, r_{global} and r_λ as the learning rates. CGA-CRN makes the candidates evolve via Selection (Line 9 of Algorithm 1), Crossover (Line 10) and Mutation (Line 11). Crossover and Mutation adopt the continuous calculation in [50]. PSO-CRN does this by updating the candidates' velocities (Line 9 of Algorithm 2) and then the candidates' positions (Line 10).

Algorithm 1 CGA for CR NOMA (CGA-CRN)

1: **Initialize**
2: Pop, r_c, r_m, and G
3: Generate the initial population $\lambda_k^{(0)}, k = 1, \ldots, Pop$
4: **for** ($g = 1$ to G) **do**
5: **for** ($k = 1$ to Pop) **do**
6: Evaluate candidate k: $\mathbf{f}_k^{(t)} = Fitness$ as in (36)
7: **end for**
8: Update the best candidates
9: Selection: reproduce the candidates
10: Crossover: pair the candidates with the rate r_c
11: Mutation: mutate the candidates with the rate r_m
12: **end for**
13: Return the best candidates

Algorithm 2 PSO for CR NOMA (PSO-CRN)

1: **Initialize**
2: Pop, G, r_{local}, r_{global}, r_λ, $\lambda_{local}^{(0)}$, λ_{global}
3: Generate the initial population of positions $\lambda_k^{(0)}$,
4: Generate the initial velocities $v_k^{(0)} = 0$ for all candidates
5: **for** ($g = 1$ to G) **do**
6: **for** ($k = 1$ to Pop) **do**
7: Evaluate candidate k: $\mathbf{f}_k^{(t)} = Fitness$ as in (36)
8: Update $\lambda_{local}^{(t)}$ and λ_{global}
9: $v_k^{(t)} = v_k^{(t)} + r_{local}(\lambda_{local}^{(t)} - \lambda_k^{(t)}) + r_{global}(\lambda_{global} - \lambda_k^{(t)})$
10: $\lambda_k^{(t)} = \lambda_k^{(t)} + r_\lambda v_k^{(t)}$
11: **end for**
12: **end for**
13: Return λ_{global}

VI. NUMERICAL RESULTS

This section examines the LP of the EAV, the OP, and the throughput of the CR NOMA system under consideration. Specifically, we analyze how the impacts of the transmit signal-to-noise ratio (SNR) of PTx_3, STx, the number of antennas of the PBS, the EAV, the channel estimation errors, the channel mean gain of PTx_3-SRx and the STx-SRx links affect the OP at the PBS, the LP at the EAV, and the throughput of the secondary network. We then compare the average generation numbers, runtimes, and average solution objective values of the CGA-CRN and PSO-CRN algorithms.

Note that we perform our analysis and simulation using

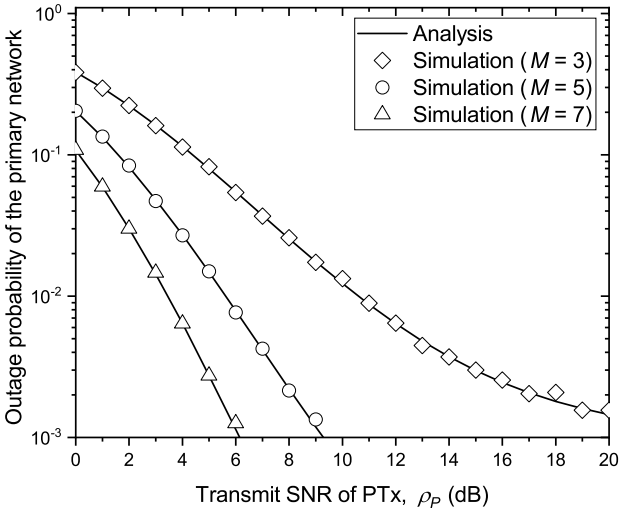

FIGURE 3: The OP at the PBS vs. the transmit power at the 3rd PTx.

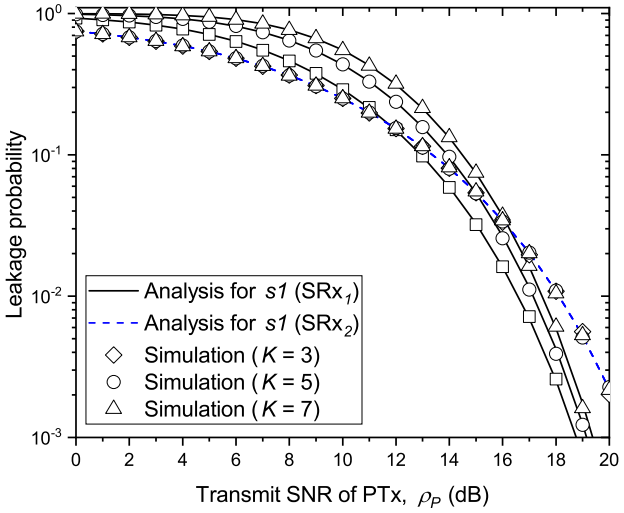

FIGURE 4: The LP at the EAV vs. the transmit power at the 3rd PTx for scheme $s1$.

the following values for all system parameters: the system bandwidth is $W = 1$ MHz; the power allocation at the STx uses $\mu_1 = 0.4$ and $\mu_2 = 0.6$; the outage target rates at the PBS, EAV, and SRxs are $R_B = 5 \times 10^5$ b/s, $R_E = 0.2 \times 10^5$ b/s, and $R_S = [10^2, 5 \times 10^3]$ b/s, respectively; the predefined threshold at the PBS is $\varepsilon_B = 10^{-2}$; the leakage threshold is $\varepsilon_E = 10^{-1}$; the numbers of PBS antennas and EAV antennas are $M, K \in \{3, 5, 7\}$; the number of PTxs is $N = 100$; the channel estimation error is $\Omega_e \in \{1, 3, 5\}$; the maximum transmit SNR at STx is $\rho_{\text{peak}} = 20$ (dB); and the transmit SNRss at the 3rd PTx and STx are $\rho_P, \rho_S \in [0, 20]$ (dB). Note that we choose $n = 3$ for the simulation, corresponding to $P_P = 12$ (dB) and $P_S^{(n)} = 11$ [4], [46], [51].

From Figures 3 to 9, the analysis curves (shown by solid and dashed lines) correspond with the simulation curves (indicated by the diamond, circle, and triangle markers), which demonstrates that our analysis is accurate.

In particular, Figure 3 illustrates the impact of the transmit SNR of the 3rd PTx ρ_P and the number of antennas of the PBS M on the OP at the PBS $\mathcal{O}_B$. The OP at the PBS decreases continuously with increasing ρ_P. This is because a high transmit power results in a high SINR value being received at the PBS. This means that the ability to decode the signal at the PBS is improved, i.e., $\mathcal{O}_B$ decreases. Furthermore, the OP at the PBS decreases when the number of antennas of this PBS increases. This is because the density gain increases with higher M.

Figure 4 presents the curve trend of the LP at the EAV $\mathcal{O}_E^{(\varphi)}$ with the transmit SNR of the 3rd PTx and the number of antennas of the EAV K for scheme $s1$. Notably, the LP approaches 1 as ρ_P decreases, and it decreases rapidly when the transmit SNR continues to increase. This means that the

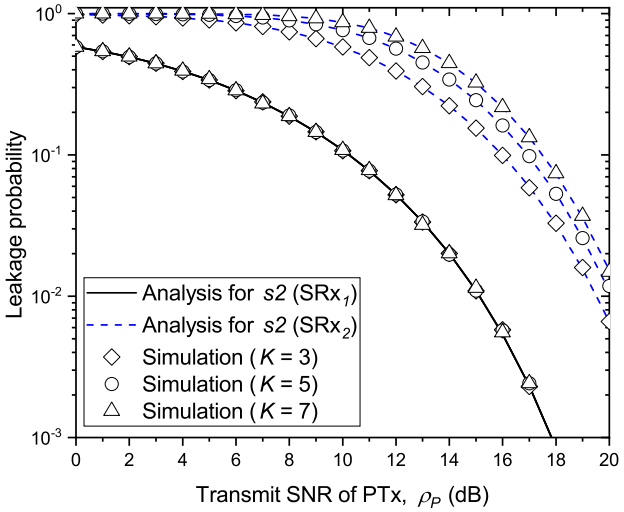

FIGURE 5: The LP at the EAV vs. the transmit power at the 3rd PTx for scheme $s2$.

EAV can more easily capture the confidential signals from the STx when $\mathcal{O}_B$ is small. This indicates that the selected 3rd PTx may yield noise for this EAV because the same channel is used. Moreover, if the number of EAV antennas increases, the LP of the first SRx's signal is higher, while the LP of the second SRx's signal will no longer change. This is because the EAV selects its optimal antenna according to the SINR of SRx_1's signal.

Similar to Figure 4, Figure 5 plots the LP at the EAV as a function of ρ_P and K for scheme $s2$. The trend is the same

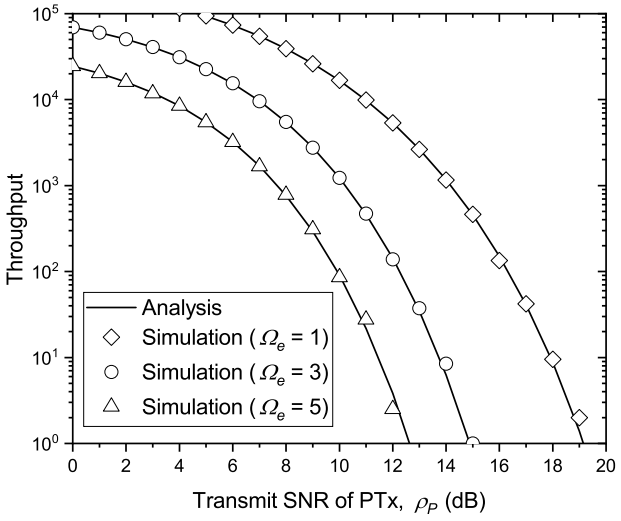

FIGURE 6: The throughput of the second network vs. the outage target rate R_S.

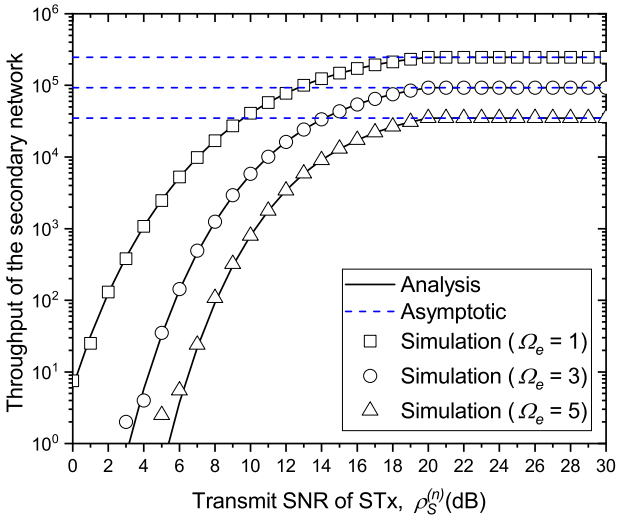

FIGURE 7: The throughput of the second network vs. the outage target rate R_S.

as in Figure 4; i.e., the LP is smaller if ρ_P is larger. However, in contrast to scheme $s1$, the LP of x_2 is improved while that of x_2 is the same when K is increased. This is because scheme $s2$ is based on the selection of the received SINR for x_2. In addition, in Figures 4 and 5, we can observe that the monitoring ability of the EAV for both signals x_1 and x_2 in scheme $s1$ is better than that in scheme $s2$.

Figure 6 depicts the throughput of the second network $\mathcal{T}_S$ versus the difference transmit power at the 3rd PTx ρ_P and the channel estimation error Ω_e. We can see that

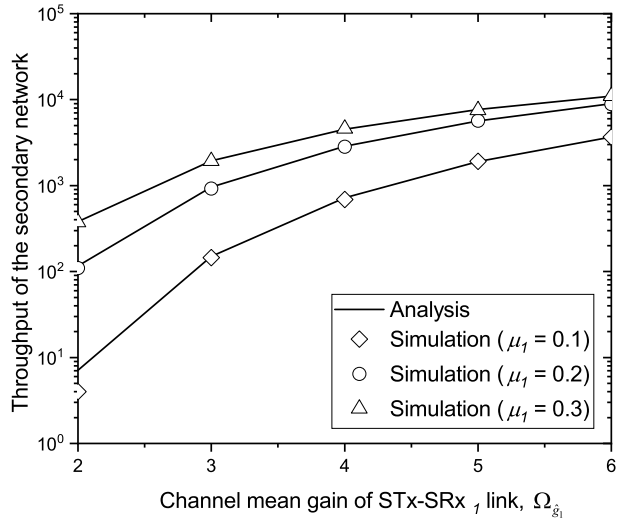

FIGURE 8: The throughput of the second network vs. the channel mean gain of the STx-SRx$_1$ link.

with the continuous increase in ρ_P, the throughput of the second network decreases continuously. This is because the CR-based secondary network's SRs experience interference from the primary network's PTx. Thus, a high ρ_P leads to a low $\mathcal{T}_S$. Furthermore, the throughput of the second network decreases gradually with increasing channel estimation error. This result can be explained by the fact that Ω_e acts as noise. Thus, a higher Ω_e leads to a lower SINRs at the SRxs, i.e., lower throughput of the second network. In contrast, as shown in Figure 7, the secondary network's throughput will rise whenever the transmit power at STx increases. Furthermore, we can see that the asymptotic outcome for the secondary network comes close to matching the corresponding simulation result in the high-SNR region. This validates our asymptotic results derived in (22), in which the asymptotic expression depends on the power allocation, outage target rate, channel estimation error, and channel mean gain of communication channels.

Figures 8 and 9 describe $\mathcal{T}_S$ with the channel mean gain of the STx-STx$_1$ link $\Omega_{\hat{g}_1}$ and the PTx$_3$-STx$_1$ link $\Omega_{\hat{f}_{n1}}$. We can see that the throughput of the second network is improved when either $\Omega_{\hat{g}_1}$ increases or $\Omega_{\hat{f}_{n1}}$ decreases. This occurs because the STx is the transmit source for the SRxs. Therefore, when $\Omega_{\hat{g}_1}$ increases, the STx will move toward STx$_1$, leading to higher channel capacity. A larger $\Omega_{\hat{f}_{n1}}$ leads to a smaller $\mathcal{T}_S$ because the STxs is noise. This trend also holds for the channel mean gain of the STx-STx$_2$ link $\Omega_{\hat{g}_2}$ and the 3rd PTx-STx$_2$ link $\Omega_{\hat{f}_{n2}}$.

Next, we initialize several parameters to apply the optimization methods described in Algorithms 1 and 2 of Section V. In particular, the population size and the limit number of generations are the same for both CGA-CRN and PSO-CRN:

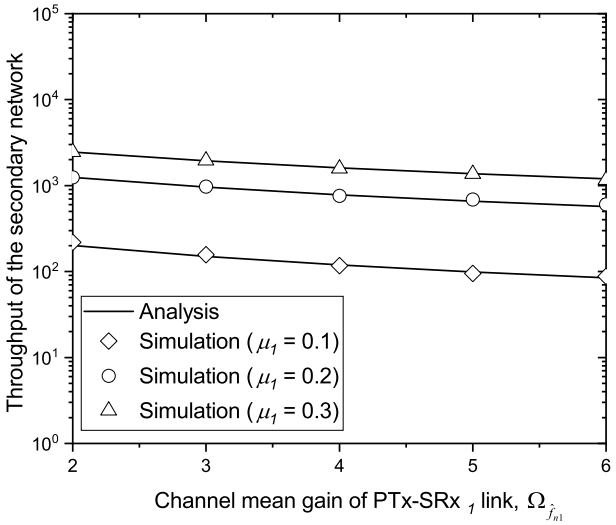

FIGURE 9: The throughput of the second network vs. the channel mean gain of the 3rd PTx-SRx$_1$ link.

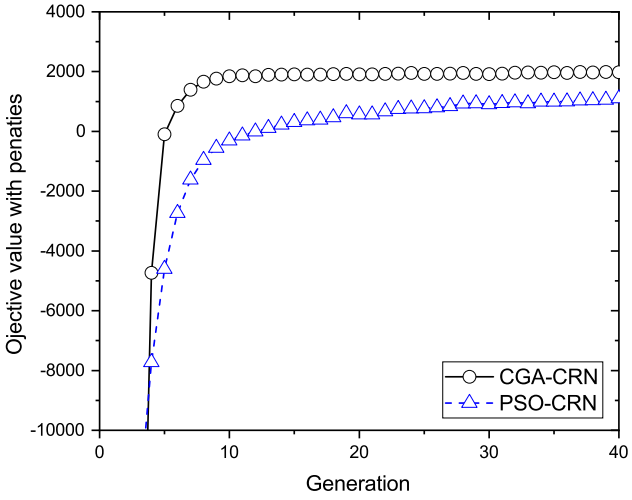

FIGURE 10: Convergence illustration for the CGA-CRN and PSO-CRN optimization methods via the average population fitness in each generation.

$Pop = 50$ and $G = 40$. For the CGA-CRN algorithm, the crossover rate is $r_c = 80\%$ and the mutation rate is $r_m = 4\%$, which means 80% of the candidates take part in the crossover step in each generation and 4% of the candidates are mutated. On the other hand, for PSO-CRN, the learning rates are $r_{local} = r_{global} = 0.3$ and $r_\lambda = 0.2$, implying that each candidate in PSO-CRN is attracted by $\lambda_{local}^{(t)}$ and λ_{global} with the same weight to refine the velocity. The algorithms are deployed on a computer with an i7-4770 CPU, a 3.40 GHz processor and 16 GB RAM in the Octave programming platform. The results are depicted in Figure 10 and Table 2.

TABLE 2: Convergence comparison details

	Average generation number to reach 95% final $Fitness$	Runtime (seconds)	Average solution's objective value
CGA-CRN	12.7	0.0625	2305.2
PSO-CRN	29.5	0.0231	2236.6

Specifically, Figure 10 demonstrates the convergence tendency of the average population fitness over the generations. Each curve illustrates the average of 100 convergence curves after 100 runs of optimization. The figure shows that the fitness of the whole population becomes increasingly high over the generations and then converges to high values in the last generations. This means the optimization works well for the problem and the best candidates found are the optimal results. It also shows that the average fitness takes negative values in the first several generations. This is because of the effect of the penalties when one or many constraints are violated. Note that for CGA-CRN, Selection is based on the round-robin wheel method [50], and the normalized versions of the fitness values must be used, which are nonnegative. Over evolution across many generations, the majority of candidates in the population can avoid the severe penalties caused by constraint violations. As a result, the average fitness of the population takes high positive values in the last generations. For more details of the convergence analysis and comparison, we added Table 2 to show how quickly convergence is achieved by CGA-CRN and PSO-CRN via the number of generations they need to converge and the runtime. These two parameters are not closely related since the average generation number needed to reach 95% the maximum $Fitness$ is the generation count regardless of how long a generation is, while the runtime values are the actual amounts of time recorded by the programs after G generations. The results in Table 2 show that CGA-CRN takes only 12.7 generations to converge, less than PSO-CRN with 29.5 generations. However, the actual runtime of PSO-CRN is better, as PSO-CRN takes approximately one-third the actual runtime of CGA-CRN. This is because CGA-CRN goes through the Selection step with the round-robin wheel algorithm, while PSO-CRN updates the candidates directly with simpler calculations. However, as a trade-off, CGA-CRN yields better final solutions, as shown in both Figure 10 and the last column of Table 2. Here, the best CGA-CRN candidates give an average throughput of 2305.2, and the best PSO-CRN candidates obtain 2236.6 with $n = 35$. Note that none of the candidates of either method violate any constraints in (34). This is obvious because PSO-CRN is more greedy and only allows candidates to move uphill toward the local best $\lambda_{local}^{(t)}$ and global best λ_{global} (see Lines 9 and 10 in Algorithm 2). Additionally, CGA-CRN is more careful and allows candidates to perform local search more efficiently with Crossover and Mutation between normal

candidates. For this optimization problem, CGA-CRN is a good choice to achieve higher objective throughput results.

VII. CONCLUSIONS

The secondary network performance in terms of the throughput of the CR NOMA systems in the presence of an EAV under imperfect CSI was investigated in this paper. Specifically, in the primary network, a PTx uses a unique channel to transmit the signal to the PBS. In the secondary network, a STx employs the NOMA technique for sending the confidential signal to the SRxs under an EAV by accessing the licensed spectrum of the primary network. Accordingly, the closed-form equation of throughput for the joint SRx_1 and SRx_2 is derived to investigate the secondary network performance. In addition, under the imperfect CSI of the channel gains, closed-form formulas are obtained for the OP at the PBS and the LP at the EAV. Then, the two algorithms (i.e., CGA-CRN and PSO-CRN) for throughput optimization are applied to guarantee the system performance of the primary network as well as the security performance of the secondary network. Next, the numerical results demonstrate that the CGA-CRN and PSO-CRN algorithms not only determine the optimal throughput but also maintain the primary network performance and prevent the secondary network's sensitive data from leaking. Finally, our CGA-CRN is suitable for solving our multiple-constraint optimization problem. However, there are some approaches that promise to improve the system performance for NOMA-CR, such as reconfigurable intelligent surfaces (RISs) [52], multihop unmanned aerial vehicle (UAV) relays [53], and blind transmission mode [54], [55]. Therefore, in future work, we will investigate deep learning to determine throughput optimization under QoS requirements for CR NOMA with a reconfigurable intelligent surface (RIS)-assisted UAV.

.

APPENDIX A PROOF OF LEMMA 1

Based on the probability characteristic, (18) can be rewritten as

$$\mathcal{O}_S = 1 - \left(1 - \underbrace{\Pr\left\{C_S^{(1)} < R_S\right\}}_{\mathcal{O}_S^{(1)}}\right) \times \left(1 - \underbrace{\Pr\left\{C_S^{(2)} < R_S\right\}}_{\mathcal{O}_S^{(2)}}\right). \quad (37)$$

Next, substituting (9) and (10) into (37), the probabilities $\mathcal{O}_S^{(1)}$ and $\mathcal{O}_S^{(2)}$ can be written as

$$\mathcal{O}_S^{(1)} = \Pr\left\{\frac{\mu_1 \rho_S^{(n)} \hat{g}_1}{\rho_P \hat{f}_{n1} + \left(\rho_S^{(n)} + \rho_P\right)\Omega_e + 1} < \theta_S\right\}, \quad (38)$$

$$\mathcal{O}_S^{(2)} = \Pr\left\{\frac{\mu_2 \rho_S^{(n)} \hat{g}_2}{\mu_1 \rho_S^{(n)} \hat{g}_2 + \rho_P \hat{f}_{n2} + \left(\rho_S^{(n)} + \rho_P\right)\Omega_e + 1} < \theta_S\right\}, \quad (39)$$

where $\theta_S = 2^{R_S/\mathrm{W}} - 1$. Then, using a similar approach to Lemma 2, $\mathcal{O}_S^{(1)}$ and $\mathcal{O}_S^{(2)}$ can be obtained by (19) and (20). The proof is complete.

APPENDIX B PROOF OF LEMMA 2

Substituting (5) and (6) into (25), we have

$$\mathcal{O}_B = \Pr\left\{\max_{1\le m\le M}\left\{\frac{\rho_P \hat{h}_{nm}}{\rho_S^{(n)} \hat{\ell}_m + \left(\rho_P + \rho_S^{(n)}\right)\Omega_e + 1}\right\} < \theta_B\right\} \le \varepsilon_B, \quad (40)$$

where $\rho_P = \frac{P_P}{N_0}$, $\rho_S^{(n)} = \frac{P_S^{(n)}}{N_0}$, and $\theta_B = 2^{R_B/W} - 1$.

Furthermore, the OP of the communication from the PTx to the PBS can be rewritten by using order statistics as follows:

$$\mathcal{O}_B = 1 - \prod_{m=1}^{M} \underbrace{\Pr\left\{\frac{\rho_P \hat{h}_{nm}}{\rho_S^{(n)} \hat{\ell}_m + 1} \ge \theta_B\right\}}_{\mathbb{P}_{\mathbb{B}}} \le \varepsilon_B. \quad (41)$$

Based on the probability characteristic and applying the PDF in (2) and the CDF in (3) for the channel gains $\hat{h}_{nm}$ and $\hat{\ell}_m$, the following probability $\mathbb{P}_{\mathbb{B}}$ can be extended after several manipulations:

$$\begin{aligned}\mathbb{P}_{\mathbb{B}} &= \Pr\left\{\hat{h}_{nm} \ge \frac{\theta_B\left(\rho_S^{(n)}\hat{\ell}_m + 1\right)}{\rho_P}\right\} \\ &= 1 - \frac{1}{\Omega_{\hat{\ell}_m}} \exp\left\{-\frac{\theta_B\left[\left(\rho_P + \rho_S^{(n)}\right)\Omega_e + 1\right]}{\rho_P \Omega_{\hat{h}_{nm}}}\right\} \\ &\quad \times \int_0^{\infty} \left\{\exp\left\{-\left(\frac{\theta_B \rho_S^{(n)}}{\rho_P \Omega_{\hat{h}_{nm}}} + \frac{1}{\Omega_{\hat{\ell}_m}}\right) u\right\}\right\} du. \quad (42)\end{aligned}$$

Finally, the integral in (42) can be calculated as (29) by applying [56, (3.310)]. The proof is complete.

APPENDIX C PROOF OF LEMMA 3

For scheme $s1$, substituting (12), (13), and (14) into (27), the leakage probabilities for decoding x_1 and x_2 are formulated as

$$\mathcal{O}_E^{(s1,1)} = 1 - \prod_{k=1}^{K} \Pr\left\{ \frac{\mu_1 \rho_S^{(n)} \hat{\beta}_k}{\rho_P \hat{\alpha}_{nk} + \left(\rho_S^{(n)} + \rho_P \Omega_e\right) + 1} < \theta_E \right\}, \quad (43)$$

$$\mathcal{O}_E^{(s1,2)} = 1 - \Pr\left\{ \frac{\mu_2 \rho_S^{(n)} \hat{\beta}_k}{\mu_1 \rho_S^{(n)} \hat{\beta}_k + \rho_P \hat{\alpha}_{nk} + \left(\rho_S^{(n)} + \rho_P\right) \Omega_e + 1} < \theta_E \right\}, \quad (44)$$

where $\theta_E = 2^{R_E/W} - 1$. Next, we can obtain $\mathcal{O}_E^{(s1,1)}$ and $\mathcal{O}_E^{(s1,1)}$ as (30) and (31) by the same approach as in Lemma 2. Furthermore, similar to scheme $s1$, the probabilities $\mathcal{O}_E^{(s2,1)}$ and $\mathcal{O}_E^{(s2,2)}$ are obtained as (32) and (33). The proof is complete.

REFERENCES

[1] A. S. Sena, F. Lima, D. Costa, Z. Ding, P. Nardelli, U. Dias, and C. Papadias, "Massive MIMO-NOMA networks with imperfect SIC: Design and fairness enhancement," *IEEE Trans. on Wireless Commun.*, vol. 19, no. 9, pp. 6100–6115, Jun. 2020.

[2] F. Fang, Y. Xu, Z. Ding, C. Shen, M. Peng, and G. K. Karagiannidis, "Optimal resource allocation for delay minimization in NOMA-MEC networks," *IEEE Trans. on Commun.*, pp. 1–15, Aug. 2020.

[3] M. Zamani, M. Eslami, M. Khorramizade, and Z. Ding, "Energy efficient power allocation for NOMA with imperfect CSI," *IEEE Trans. Veh. Technol.*, vol. 68, no. 1, pp. 1009–1013, Jan. 2019.

[4] D.-T. Do, M. Vaezi, and T.-L. Nguyen, "Wireless powered cooperative relaying using NOMA with imperfect CSI," in *Proc. IEEE Globecom*, Abu Dhabi, U.A.E, Sep. 2018, pp. 1–6.

[5] K. Higuchi and A. Benjebbour, "Non-orthogonal multiple access (NOMA) with successive interference cancellation for future radio access," *IEICE Trans. commun.*, vol. E98-B, no. 3, pp. 403–414, Mar. 2015.

[6] V. N. Vo, C. So-In, D.-D. Tran, and H. Tran, "Optimal system performance in multihop energy harvesting WSNs using cooperative NOMA and friendly jammers," *IEEE Access*, vol. 7, pp. 125 494–125 510, Sep. 2019.

[7] Z. Chen, Z. Ding, X. Dai, and R. Zhang, "A mathematical proof of the superiority of NOMA compared to conventional OMA," *IEEE Trans. Signal Process.*, pp. 1–28, Oct. 2016.

[8] H. Tabassum, M. A. end E. Hossain, M. Hossain, and D. I. Kim, "Uplink vs. downlink NOMA in cellular networks: Challenges and research directions," in *Proc. IEEE Vehicular Tech. Conf.* Sydney, N.S.W., Australia, Jun. 2017, pp. 1–7.

[9] X. Tian, Q. Li, X. Li, H. P. 1, C. Zhang, K. M. Rabie, and R. Kharel, "I/Q imbalance and imperfect SIC on two-way relay NOMA systems," *Electronics*, vol. 9, no. 249, pp. 1–16, Feb. 2020.

[10] L. Lv, J. Chen, Q. Ni, Z. Ding, and H. Jiang, "Cognitive non-orthogonal multiple access with cooperative relaying: A new wireless frontier for 5G spectrum sharing," *IEEE Commun. Magazine*, vol. 56, no. 4, pp. 188–195, Apr. 2018.

[11] S. Guo and X. Zhou, "Robust resource allocation with imperfect channel estimation in NOMA-based heterogeneous vehicular networks," *IEEE Trans. Commun.*, vol. 67, no. 3, pp. 2321–2332, Mar. 2019.

[12] D.-T. Do, A.-T. Le, and B. M. Lee, "NOMA in cooperative underlay cognitive radio networks under imperfect SIC," *IEEE Access*, vol. 8, pp. 86 180–86 195, May 2020.

[13] B. Alzahrani and W. Ejaz, "Resource management for cognitive IoT systems with RF energy harvesting in smart cities," *IEEE Access*, vol. 6, pp. 62 717–62 727, Oct. 2018.

[14] D.-T. Do, A.-T. Le, and B. M. Lee, "On performance analysis of underlay cognitive radio-aware hybrid OMA/NOMA networks with imperfect CSI," *Electronics*, vol. 8, no. 7, pp. 1–21, Jul. 2019.

[15] D.-T. Do, A.-T. Le, C.-B. Le, and B. M. Lee, "On exact outage and throughput performance of cognitive radio based non-orthogonal multiple access networks with and without D2D link," *Sensors*, vol. 19, no. 15, pp. 1–17, Jul. 2019.

[16] L. Lv, J. Chen, and Q. Ni, "Cooperative non-orthogonal multiple access in cognitive radio," *IEEE Commun. Letters*, vol. 20, no. 10, pp. 2059–2062, Oct. 2016.

[17] Z. Xiang, W. Yang, G. Pan, Y. Cai, and Y. Song, "Physical layer security in cognitive radio inspired NOMA network," *IEEE J. of Selected Topics in Signal Processing*, vol. 13, no. 3, pp. 700–714, Jul. 2019.

[18] Y. Zou, B. Champagne, W.-P. Zhu, and L. Hanzo, "Relay-selection improves the security-reliability trade-off in cognitive radio systems," *IEEE Trans. Commun.*, vol. 63, no. 1, pp. 215–228, Jan. 2015.

[19] N. Mokari, S. Parsaeefard, H. Saeedi, P. Azmi, and E. Hossain, "Secure robust ergodic uplink resource allocation in relay-assisted cognitive radio network," *IEEE Trans. Signal Process.*, vol. 63, no. 2, pp. 291–304, Jan. 2015.

[20] T.-P. Huynh, P. N. Son, and M. Voznak, "Secrecy performance of underlay cooperative cognitive network using non-orthogonal multiple access with opportunistic relay selection," *Symmetry*, vol. 11, no. 3, pp. 1–17, Mar. 2019.

[21] H. M. A. Abdullah and A. V. S. Kumar, "HFSA-SORA: Hybrid firefly simulated annealing based spectrum opportunistic routing algorithm for cognitive radio Ad hoc networks (crahn)," in *proc. Intern. Conf. Intelligent Comput. and Control*, Jun. 2017, pp. 1–10.

[22] F. Okoli, J. Bert, S. Abdelaziz, N. Boussion, and D. Visvikis, "Optimizing the beam selection for noncoplanar VMAT by using simulated annealing approach," *IEEE Trans. Radiation Plasma Medical Sci.*, vol. 6, no. 5, pp. 609–618, May 2022.

[23] D. K. Luong, M. Ali, Y. F. Hu, J. P. Li, R. Asif, and K. Abdo, "Simulated annealing-based multilink selection algorithm in SDN-enabled avionic networks," *IEEE Access*, vol. 9, pp. 145 301–145 316, Oct. 2021.

[24] A. M. Yesaswini and K. Annapurna, "GA and PSO based spectrum allotment in cognitive radio networks," in *Intern. Conf. Inventive Computat. Techn.*, Feb. 2021, pp. 701–704.

[25] M. G. C. P and V. T, "Analysis and performance evaluation of PSO for spectrum allocation in CRN," in *Intern. Conf. Innovative Practices Techno. and Management*, Apr. 2021, pp. 119–124.

[26] D.-T. Do, A.-T. Le, and B. M. Lee, "NOMA in cooperative underlay cognitive radio networks under imperfect SIC," *IEEE Access*, vol. 8, pp. 86 180–86 195, May 2020.

[27] M. Qin, S. Yang, H. Deng, and M. H. Lee, "Enhancing security of primary user in underlay cognitive radio networks with secondary user selection," *IEEE Access*, vol. 6, pp. 32 624–32 636, Jun. 2018.

[28] K. Mehr, J. Niya, H.Seyedarabi, and S. Nobar, "Secrecy capacity results for a secure NOMA-based cognitive radio network with an external eavesdropper," *IEEE Trans. Commun.*, vol. 43, Dec. 2020.

[29] Z. Xiang, W. Yang, Y. Cai, Z. Ding, and Y. Song, "Secure transmission design in HARQ assisted cognitive NOMA networks," *IEEE Trans. Inf. Forensics Secur.*, vol. 15, pp. 2528–2541, Jan. 2020.

[30] M. Zeng, W. Hao, O. A. Dobre, Z. Ding, and H. V. Poor, "Power minimization for multi-cell uplink NOMA with imperfect SIC," *IEEE Wireless Communications Letters*, vol. 9, no. 12, pp. 2030–2034, 2020.

[31] N. Tang, H. Tang, B. Li, and X. Yuan, "Cognitive NOMA for UAV-enabled secure communications: Joint 3d trajectory design and power allocation," *IEEE Access*, vol. 8, pp. 159 965–159 978, 2020.

[32] J. Kwak and N. B. Shroff, "Simulated annealing for optimal resource allocation in wireless networks with imperfect communications," in *2018 56th Annual Allerton Conference on Communication, Control, and Computing (Allerton)*, 2018, pp. 903–910.

[33] L. Yang, F. Zhu, X. Liu, W. Lai, W. Li, and S. Lyu, "Enhanced bat algorithm for resource allocation in wireless heterogeneous networks," in *2021 31st International Telecommunication Networks and Applications Conference (ITNAC)*, 2021, pp. 98–103.

[34] S. Anil, M. Pappa, and C. Ramesh, "Implementation of MIMO OFDM NOMA system using iterative algorithm," *IOP Conference Series: Materials Science and Engineering*, vol. 1166, no. 1, pp. 12–42, jul 2021.

[35] B. Ji, Y. Li, S. Chen, C. Han, C. Li, and H. Wen, "Secrecy outage analysis of UAV assisted relay and antenna selection for cognitive network under nakagami-m channel," *IEEE Trans. on Cognitive Commun. and Networking*, vol. 7, pp. 1–11, Jan. 2020.

[36] B. Ji, Y. Li, B. Zhou, C. Li, K. Song, and H. Wen, "Performance analysis of UAV relay assisted IoT communication network enhanced with energy harvesting," *IEEE Access*, vol. 7, pp. 38 738–38 747, 2019.

[37] X. Cao, X. Wang, and X. Lin, "Design and implementation of a centralized routing protocol for wireless sensor network," in *Proc. Int. Conf. Sensing Tech.*, Nov. 2016, pp. 1–6.

[38] Y. He and S. Dey, "Secrecy capacity of wireless channels," *IEEE Trans. on Commun.*, vol. 59, no. 6, pp. 1644–1656, Jun. 2011.

[39] T. H. Pham, X. J. Li, P. H. J. Chong, and Y. W. Leong, "Design and implementation of a centralized routing protocol for wireless sensor network," in *Proc. Int. Conf. Commun. Software and Net.*, Nov. 2010, p. 88–92.

[40] H. Tran, T. X. Quach, H. Tran, and E. Uhlemann, "Optimal energy harvesting time and transmit power in cognitive radio network under joint constraints of primary users and eavesdroppers," in *Proc. Int. Symp. on Personal, Indoor and Mobile Radio Commun.*, Oct. 2017, pp. 1–8.

[41] D. Sun, T. Song, B. Gu, X. Li, J. Hu, and M. Liu, "Spectrum sensing and the utilization of spectrum opportunity tradeoff in cognitive radio network," *IEEE Commun. Letters*, vol. 20, no. 12, pp. 2442–2445, Dec. 2016.

[42] H. V. Toan, V. N. Q. Bao, and H. N. Le, "Cognitive two-way relay systems with multiple primary receivers: exact and asymptotic outage formulation," *IET Commun.*, vol. 11, no. 16, pp. 2490–2497, Nov. 2017.

[43] Y. Deng, M. Elkashlan, P. L. Yeoh, N. Yang, and R. K. Mallik, "Cognitive mimo relay networks with generalized selection combining," *IEEE Trans. Wireless Commun.*, vol. 13, no. 9, pp. 4911–4922, Sep. 2014.

[44] C. Guo, L. Zhao, C. Feng, Z. Ding, and H.-H. Chen, "Energy harvesting enabled NOMA systems with full-duplex relaying," *IEEE Trans. Veh. Technol.*, vol. 68, no. 7, pp. 7179–7183, Jul. 2019.

[45] X. Song, L. Dong, J. Wang, L. Qin, and X. Han, "Energy efficient power allocation for downlink NOMA heterogeneous networks with imperfect CSI," *IEEE Access*, vol. 7, pp. 39 329–39 340, Mar. 2019.

[46] V. N. Vo, T. G. Nguyen, C. So-In, and H. Tran, "Outage performance analysis of energy harvesting wireless sensor networks for NOMA transmissions," *Mobile Networks and Applicat.*, vol. 25, pp. 23–41, Jan. 2020.

[47] V. N. Vo, C. So-In, H. Tran, D.-D. Tran, S. Heng, P. Aimtongkham, and A.-N. Nguyen, "On security and throughput for energy harvesting untrusted relays in IoT systems using NOMA," *IEEE Access*, vol. 7, pp. 149 341–149 354, Oct. 2019.

[48] H. Lee, C. Song, S. H. Choi, and I. Lee, "Outage probability analysis and power splitter designs for SWIPT relaying systems with direct link," *IEEE Commun. Lett.*, vol. 21, no. 3, pp. 648–651, Mar. 2017.

[49] B. C. Nguyen, N. N. Thang, T. M. Hoang, and L. T. Dung, "Analysis of outage probability and throughput for energy harvesting full-duplex decode-and-forward vehicle-to-vehicle relay system," *Wireless Commun. and Mobile Computing*, vol. 2020, pp. 1–10, May 2020.

[50] R. L. Haupt and S. E. Haupt, *Practical Genetic Algorithms*. John Wiley & Sons, 2004.

[51] Y. Chen, N. Zhao, and Z. D. M.-S. Alouini, "Multiple UAVs as relays: Multi-hop single link versus multiple dual-hop links," *IEEE Trans. Wireless Commun.*, vol. 17, no. 9, pp. 6348–6359, Aug. 2018.

[52] W. Liang, W. Luo, J. Zhang, and Z. Ding, "Active and passive beamforming design for reconfigurable intelligent surface assisted CR-NOMA networks," *IEEE Commun. Letters*, vol. 26, no. 10, pp. 2409–2414, 2022.

[53] V. H. D. *et al.*, "Throughput optimization for noma energy harvesting cognitive radio with multi-uav-assisted relaying under security constraints," *IEEE Trans. Cognitive Commun. and Networking*, pp. 1–1, 2022.

[54] H. Yahya, A. Al-Dweik, E. Alsusa, and M. Debbah, "Priority-based dynamic IoT-downlink communications with blind transmission-mode recognition," *IEEE Internet of Things Magazine*, vol. 5, no. 3, pp. 106–112, 2022.

[55] H. Yahya, E. Alsusa, and A. Al-Dweik, "Blind receiver design for downlink cognitive-radio NOMA networks," in *IEEE Intern. Conf. Commun. Workshops*, 2021, pp. 1–6.

[56] I. Gradshteyn and I. Ryzhik, *Table of Integrals, Series, and Products*, 8th ed., D. Zwillinger and V. Moll, Eds. Elsevier, 2014.

VAN NHAN VO is currently a lecturer at Duy Tan University, Vietnam. He received his B.S., M.S., and Ph.D. degrees in Computer Science from the University of Da Nang and Duy Tan University in Da Nang, Vietnam, and from Khon Kaen University, Thailand, in 2006, 2014, and 2019, respectively. His research interests include optimization, information security, physical-layer secrecy, radio frequency energy harvesting, nonorthogonal multiple access, wireless sensor networks, the Internet of Things, unmanned aerial vehicles, and the security of other advanced communication systems.

VIET-HUNG DANG completed his B.S. and M.S. degrees at Ho Chi Minh University of Technology, Vietnam, in 2005 with a background in Electronics and Telecommunications. He received a Ph.D. degree in Computer Science from Kyung Hee University, Korea, in 2012 and has been working at Duy Tan University, Vietnam, since then. His research interests include wireless networks, distributed computing, optimization, supervised machine learning, and reinforcement learning.

HUNG TRAN received his B.S. and M.S. degrees in Information Technology from Vietnam National University, Hanoi, in 2002 and 2006, respectively, and his Ph.D. degree from the School of Computing, Blekinge Institute of Technology, Karlskrona, Sweden, in 2013. He is currently a lecturer in the Faculty of Computer Science, Phenikaa University, Yen Nghia Ward, Ha Dong District, Hanoi, Vietnam, and a postdoctoral researcher with Mälardalen University, Sweden. His research interests include cognitive radio networks, cooperative communication systems, millimeter wave communications, energy harvesting and secure communications in the physical layer. He is also a cocreator of the Academic Gates platform, which helps research labs and universities recruit talent (https://www.academicgates.com).

DAC-BINH HA received his B.S. degree in Radio Techniques and his M.S. and Ph.D. degrees in Communications and Information Systems from Huazhong University of Science and Technology (HUST), China in 1997, 2006, and 2009, respectively. He is currently the Dean of the Faculty of Electrical and Electronics Engineering, Duy Tan University, Vietnam. His research interests include information security, physical-layer secrecy, radio frequency energy harvesting, nonorthogonal multiple access, wireless sensor networks, the Internet of Things, and mobile edge computing.

CONG LE is currently a lecturer in the Faculty of Computer Science, Vietnam Korea University of Information and Communications Technology, Danang University, Vietnam. He received his B.S. and M.S. degrees in Computer Science from the University of Danang - University of Science and Education, Danang, and the University of Science and Technology of Hanoi in 2005 and 2012, respectively. His research interests include physical layer security, NOMA networks, and cognitive radio networks.

TU DAC HO has been an Associate Professor in the Department of Electrical Engineering at the Arctic University of Norway (UiT) since 2019. Dr. Ho received M.S. and Ph.D. degrees from Waseda University in Tokyo, Japan, in 2005 and 2011, respectively, both in wireless communications. Before working at UiT, he was an Assistant Professor at the Global Information and Telecommunication Institute (GITI), Waseda University of Japan (2011–2012); a postdoctoral fellow at the Norwegian University of Science and Technology (2012–2014), and a senior researcher at SINTEF Norway (2014–2018). Dr. Ho has participated in and led several scientific projects in Norway and Europe focusing on, e.g., communications in the Arctic and the applications of unmanned aerial vehicles in autonomous systems focused on monitoring/surveillance/networking and decision support for operations in the Arctic and other remote regions. His research interests include communications and networking, communication protocols, the Internet of Things, wireless sensor networks, cyber-physical systems, network/system optimization, and communications/path planning for intelligent unmanned systems. He has served as a committee member/reviewer for many journals from publishers such as IEEE, Elsevier, Springer, Wiley, IET, IEICE, and AIAA and for conferences such as GLOBECOM, ICC, VTC, WCNC, CCNC, ICUAS, and PIMRC. Dr. Ho is a member of IEEE.

CHAKCHAI SO-IN is a Professor of Computer Science in the Department of Computer Science, Khon Kaen University, KK, TH. He received B.Eng./M.Eng. degrees from Kasetsart University, BKK, TH in 1999/2001 and M.S./Ph.D. degrees from Washington University in St. Louis, MO, USA in 2006/2010, all in Computer Engineering. He has interned with Cisco Networking Academy (CNAP-NTU, SG), Cisco Systems (Silicon Valley, USA), WiMAX Forums (USA), and Bell Labs (Alcatel-Lucent, USA). His research interests include computer networking and the internet, wireless and mobile networking, the Internet of Things, wireless sensor networks, signal processing, cybersecurity, cyber-physical systems, and applied intelligent systems. He has served as an associate editor for IEEE Access, PLOS ONE, Wireless Networks, WCMC, PeerJ (CS), and ECTI-CIT and as a committee member/reviewer for many journals/publishers such as IEEE, Elsevier, Springer, Wiley, IET, Inderscience, IEICE, and ETRI as well as conferences such as GLOBECOM, ICC, VTC, WCNC, ICNP, ICNC, and PIMRC. He has authored or coauthored over 100 international (technical) publications, including some in IEEE JSAC, IEEE TCCN, IEEE/CAA, IEEE Commun./Wireless Commun. Mags, IEEE IoT J., IEEE System J., COMNET, MONET, and ESWA, and 10 books, including Mobile & Wireless Nets with IoT, Computer Network Lab., and Network Security Lab. He is also a senior member of IEEE and ACM.